JOURNAL OF MECHANICAL ENGINEERING AND SCIENCES
ISSN: 2289-4659 e-ISSN: 2231-8380
VOLUME 19, ISSUE 3, 2025, 10713 - 10726
DOI: https://doi.org/10.15282/jmes.19.3.2025.2.0840

RESEARCH ARTICLE

Simultaneous humidity and temperature measurement sensor based on coated multiplexed fibre Bragg gratings

A. R. Azmi[1], A. M. Aizzuddin[1], E. Vorathin[1]*, K. S. Lim[2], M. Mohammad[1], A. R. Othman[1], A. R. Ismail[3]

[1] Department of Mechanical Engineering, Universiti Teknologi PETRONAS, 32610 Seri Iskandar, Perak Darul Ridzuan, Malaysia
Phone: +605-3687197; Fax.: +605-3656461
[2] Photonics Research Centre, University of Malaya, 50603, Kuala Lumpur, Malaysia
[3] College of Health Sciences, University of Sharjah, P.O. Box 27272, Sharjah, United Arab Emirates

ABSTRACT – Fibre Bragg Grating (FBG) sensors are preferred over traditional electrical sensors due to their high sensitivity, electromagnetic immunity, and multiplexing capability. However, the simultaneous measurement of humidity and temperature remains challenging due to cross-sensitivity issues. This study presents the development of an efficient and straightforward coated multiplexed FBG sensor to address this challenge. The sensor was fabricated using two separate single-mode fibre FBGs, each coated with polydimethylsiloxane (PDMS) and polyvinyl alcohol (PVA), respectively. Experimental results demonstrated that PDMS exhibited excellent temperature sensitivity, while PVA showed high moisture sensitivity. The measured sensitivities were 0.0989 pm/% RH (equivalent to 9.89 pm.φ^{-1}) and 28.775 pm/°C (equivalent to 28.775 pm/°K) for PDMS-coated FBG, and 12.593 pm/% RH and 14.515 pm/°C for PVA-coated FBG, indicating that PDMS had minimal response to humidity. In contrast, PVA exhibited a degree of temperature sensitivity. To mitigate cross-sensitivity, a sensitivity matrix was employed, allowing for the accurate simultaneous measurement of humidity and temperature. The experimental validation confirmed that the sensor achieved a percentage error of less than 10%, demonstrating high accuracy and reliability. Given the simplicity of fabrication and calibration, the proposed coated multiplexed sensor exhibits strong potential for practical applications in environmental monitoring and industrial sensing.

ARTICLE HISTORY
Received : 12th Mar. 2025
Revised : 09th July 2025
Accepted : 04th Sept. 2025
Published : 30th Sept. 2025

KEYWORDS
Humidity and temperature
FBGs
Simultaneous measurement
Coated FBGs
Multiplexed
Sensitivity matrix

1. INTRODUCTION

Accurate monitoring of environmental parameters is crucial across various industries, including agriculture and healthcare [1, 2]. Among these parameters, humidity and temperature have a significant influence on material properties, equipment performance, and overall system efficiency [3, 4]. Fibre Bragg Grating (FBG) sensors have gained attention due to their inherent advantages, including high sensitivity, electromagnetic immunity, and the ability to be multiplexed along a single optical fibre [5, 6], unlike traditional electric sensors. However, simultaneous measurement of humidity and temperature using FBG sensors remains challenging due to cross-sensitivity effects [7]. One promising approach to overcome this challenge involves using coatings that enhance the sensor's responsiveness to humidity while ensuring accurate temperature measurement. Han et al. [8] proposed a method using two long-period fibre gratings (LPFGs) coated with humidity-sensitive material, polyimide and graphene quantum dots (PI+GQDs), and temperature-sensitive material, dimethyl silicone oil (DSO), on the surface. The sensors achieved sensitivities of 78 pm/% RH and 445 pm/°C, for humidity and temperature, respectively. However, the proposed sensors require advanced fabrication techniques, making their implementation challenging. Similarly, Tong et al. [9] developed a sensor based on a compact Mach-Zehnder interferometer and a Fabry-Pérot interferometer, achieving sensitivities of -132 pm/% RH for humidity and 370 pm/°C for temperature, with resolutions of 0.15% RH and 0.05°C, respectively. While this approach demonstrated promising performance, it also necessitates in-depth knowledge of the sensing principle and advanced practical skills in handling optical fibres, limiting its accessibility. Moreover, despite their high sensitivity, Mach-Zehnder and Fabry-Perot interferometers face challenges in multiplexing, and the reflective mirrors in the Fabry-Perot interferometer require precise alignment to minimize coupling loss [10].

Alternatively, Qi et al. [11] developed a simpler cascaded grating sensor with a film-modified LPFG and FBG coated with polyvinyl alcohol (PVA) on the surface of the LPFG. This design achieved sensitivities of 34.99 pm/% RH and 94.34 pm/°C, for humidity and temperature, respectively. This design offers a more straightforward structure compared to previous approaches. These studies highlight the ongoing research in developing effective methods for simultaneous humidity and temperature measurement, with a focus on improving sensor sensitivity, structural simplicity, and ease of fabrication. Recent advancements have introduced alternative designs to simplify the fabrication process while simultaneously measuring humidity and temperature. Cheng et al. [12] proposed a design that requires only a magnetron sputtering operation for sensor coating, thereby significantly simplifying the fabrication process. Their approach involves inserting a no-core optical fibre (NCF) between two multimode optical fibres (MMF), forming an MMF-NCF-MMF

*CORRESPONDING AUTHOR | E. Vorathin | ✉ vorathin.epin@utp.edu.my

structure. However, this design is primarily intended for measuring ultraviolet irradiance and temperature rather than humidity. Fan et al. [13] explored a polymeric microwire-enabled FBG for simultaneous measurement of relative humidity (RH) and temperature. Their sensor achieved sensitivities of 360.8 pm/% RH and -120 pm/°C, respectively. The authors mentioned that FBGs do not respond to the surrounding humidity perturbation due to their location in the fibre core and demonstrate a temperature sensitivity of 10 pm/°C. This indicates that FBGs can be used strategically to eliminate temperature-induced cross-sensitivity in humidity measurements, enabling accurate simultaneous sensing of humidity. Zhang et al. [14] addressed the cross-sensitivity challenge by utilizing two different materials: polydimethylsiloxane (PDMS) and a blend of eosin Y, methyldiethanolamine (MDEA), and pentaerythritol triacrylate (PETA), which forms a photopolymer. This combination generated two spectral frequency ranges with different sensitivities to humidity and temperature fluctuations, effectively enabling simultaneous measurement while mitigating temperature-humidity crosstalk. The achieved sensitivities of humidity and temperature were 282 pm/% RH and 1880 pm/°C, respectively, demonstrating the effectiveness of this approach.

Beyond these designs, various other methodologies have been explored to enhance simultaneous humidity and temperature sensing. Researchers have investigated techniques such as forward Brillouin scattering (BLS) in the fibre [15], optical frequency domain reflectometry (OFDR) with a single-sensing fibre configuration [16], and an asymmetric single-mode-multimode-single-mode interferometer processed via a femtosecond laser system [17]. Additional approaches include a fibre-tip microcantilever cascaded with FBG [18] and a graphene oxide (GO)-coated loop fibre integrated with an FBG [19]. Each of these techniques introduces unique advantages in sensor design and measurement accuracy. Despite these advancements, research on simultaneous humidity and temperature sensing using two coated FBGs spliced together remains limited. The gap presents an opportunity to explore FBG-based dual-coating strategies that enhance sensitivity, reduce cross-sensitivity, and simplify sensor fabrication, contributing to further improvements in environmental monitoring applications. Hence, this study aims to develop a simple coated multiplexed FBG sensor system capable of accurately measuring both humidity and temperature. The sensor's performance was evaluated under controlled laboratory conditions to determine its sensitivity and accuracy. By utilizing the wavelength-encoded sensing capabilities of FBGs and integrating specialized coatings, this research aims to enhance the efficiency of simultaneous humidity and temperature measurement, addressing critical challenges in optical fiber sensing technology.

2. MATERIALS AND METHODS

2.1 Fabrication of Coated Multiplexed FBG Sensor

The proposed humidity and temperature sensor comprises a multiplexed FBG sensor spliced with three gratings, each 10 mm in length. In this experiment, PDMS and PVA were used to coat the grating regions corresponding to Bragg wavelengths of 1549 nm and 1554 nm, respectively. The FBG with a wavelength of 1539 nm remained uncoated as a reference. The PDMS solution was prepared using the SYLGARD™ 184 Silicone Elastomer Kit by mixing the base and curing agent at a mass ratio of 10:1. To enhance PDMS adhesion to the fibre surface, (3-Aminopropyl) trimethoxysilane (APTMS) was added to a methanol solution with a 4% APTMS concentration. Meanwhile, PVA powder was dissolved in deionised water to obtain a 5% PVA solution. Both coatings were applied using a dip-coating technique to ensure uniform coverage on the designated FBGs. The FBGs were then spliced together to form the multiplexed coated FBG sensor, as illustrated in Figure 1(a). Additionally, an uncoated FBG was included in the setup to serve as a reference for temperature compensation. Figure 1(b) presents a schematic representation of the fabricated coated multiplexed sensor.

The working principle of FBG sensors is based on periodic modulations in the refractive index of the fibre core, which selectively reflect specific wavelengths of light [20]. FBG sensors are fabricated by inducing a periodic variation in the core's refractive index, forming a grating structure. The reflected wavelength, known as the Bragg wavelength, is determined by the grating period and the refractive index of the fibre core. Fibre sensors are highly sensitive to both strain and temperature. Strain affects the grating period by physically elongating or compressing the fibre, leading to a shift in the Bragg wavelength. Temperature variations influence both the refractive index and the grating spacing due to thermal expansion and the thermo-optic effect, resulting in an additional wavelength shift [21]. The wavelength shifts serve as the fundamental sensing mechanism in FBG-based measurements. The Bragg wavelength shift, $\Delta\boldsymbol{\lambda}_{\mathrm{B}}$, can be mathematically expressed as [22]:

$$\frac{\Delta\lambda_B}{\lambda_B} = (1 - P_e)\Delta\varepsilon + (\,\hat{a} + \xi)\Delta T \tag{1}$$

where, $\Delta\lambda_B$ is the Bragg wavelength shiftλ_B is the initial central wavelength, â is the coefficient of thermal expansion for the fibre, ξ is the thermo-optic coefficient of the fibre material, P_e is the effective strain-optic coefficient, ΔT is the temperature variation, $\Delta\varepsilon$ is the applied strain

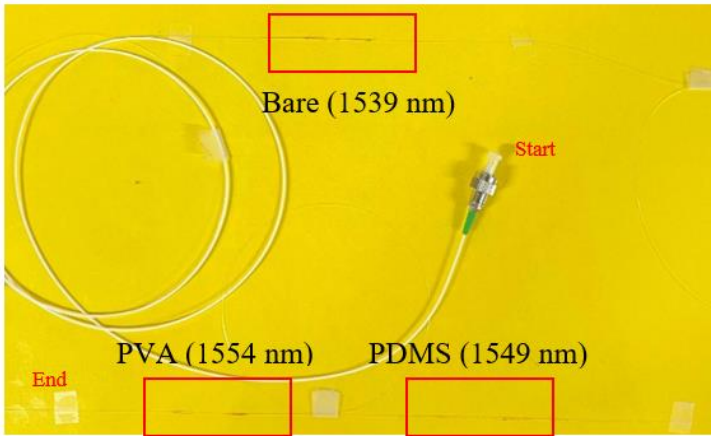

(a)

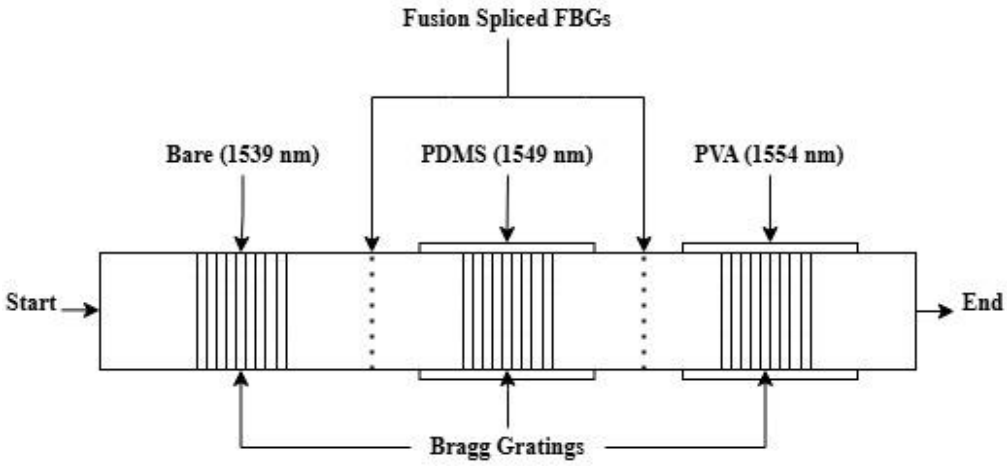

(b)

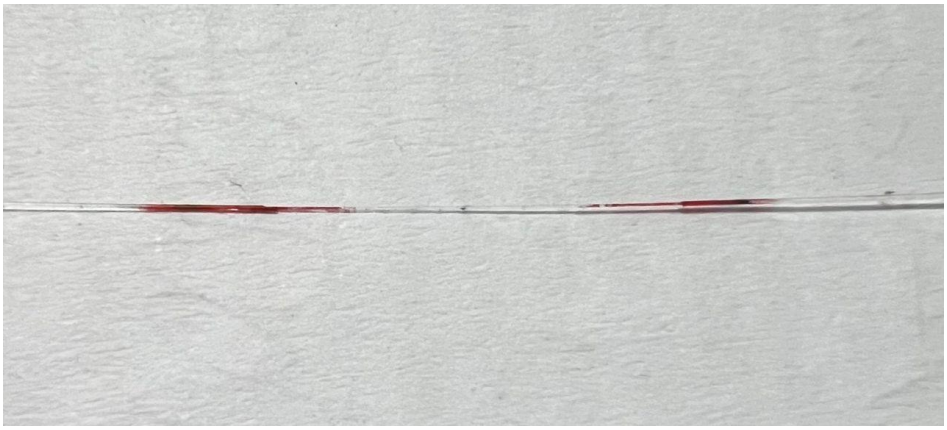

(c)

Figure 1. (a) Actual FBG, (b) schematic of fabricated coated multiplexed FBG sensor and (c) zoomed in sample of coated FBG with red highlights between coating area

This experiment focuses on the simultaneous measurement of humidity and temperature, with Eq. (1) explaining the working principle of a single FBG sensor. The proposed sensor system consists of two coated FBGs spliced together, along with a bare FBG included as a reference for performance comparison. A key challenge in simultaneous measurements is cross-sensitivity, particularly temperature-induced interference. To address this issue, a sensitivity matrix was employed to decouple the effects of temperature and humidity, ensuring accurate measurements. The sensitivity matrix can be expressed as:

$$\begin{bmatrix} \Delta\lambda_{B1} \\ \Delta\lambda_{B2} \end{bmatrix} = \begin{bmatrix} S_{11} & S_{12} \\ S_{21} & S_{22} \end{bmatrix} \begin{bmatrix} \Delta\varepsilon \\ \Delta T \end{bmatrix} \quad (2)$$

where, S_{11} and S_{12} are the strain and temperature sensitivities of $\Delta\lambda_{B1}$, whereas S_{21} and S_{22} are the strain and temperature sensitivities of $\Delta\lambda_{B2}$.

2.2 Relative Humidity Calibration

Based on Eq. (1), RH induces strain on the grating period due to the hydrophilic nature of the PVA coating. Therefore, it is crucial to calibrate the RH-induced strain on the FBGs while maintaining the temperature at 26 °C ± 0.2 °C or equivalent to 299.15 °K ± 0.2 °K. To regulate RH levels, different types of saturated salt solutions were used. The experimental setup for RH calibration is illustrated in Figure 2. A sealed container with a tight lid was used to maintain a stable humidity environment, and a thermo-hygrometer was placed inside to monitor temperature and RH. The optical spectrum analyser (OSA), manufactured by Ibsen Photonics (model I-MON 256 USB), and a broadband light source (BLS) model DL-BP1 1501A, along with an optical circulator, were utilised in the experiment. The broadband light source transmitted light through the grating regions of the coated multiplexed FBG sensor. Changes in RH caused expansion in the coating materials, inducing strain on the fibre, which altered the grating period. This modification in the grating period resulted in shifts in the transmitted light, which was then reflected into the optical circulator. The circulator directed the reflected light to the OSA for spectral analysis. The optical spectrum analyzer has a wavelength resolution of less than 0.0005 nm and a repeatability of 0.003 nm, with a maximum uncertainty of 0.005 nm. Hence, precise data measurement can be obtained.

The experiment was conducted on the multiplexed FBG coated with PDMS and PVA to evaluate its sensitivity to humidity. The data measurement was repeated three times to obtain an average of the results. Saturated salt solutions were used to create a controlled humidity environment at different RH levels, with corresponding RH values recorded from the thermo-hygrometer. The RH levels generated by the different salt solutions were based on values reported by Greenspan [23], as shown in

Table 1. The measured data were used to calibrate the sensor and determine its RH sensitivity.

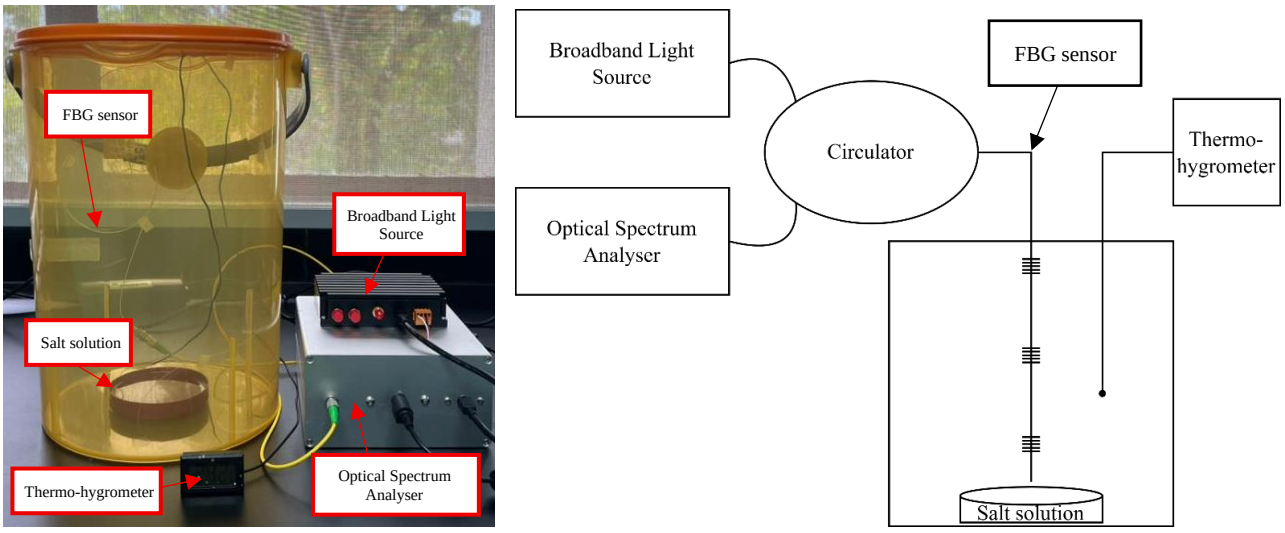

Figure 2. Actual and schematic experiment setup of relative humidity calibration

Table 1. Relative humidity of the salt solution, reported in %RH (φ = %RH/100, dimensionless fraction)

Salt solution	Relative humidity (% RH;φ)
Potassium sulfate (K_2SO_4)	95
Potassium chloride (KCl)	85
Ammonium nitrate (NH_4NO_3)	77
Potassium carbonate (K_2CO_3)	56
Magnesium chloride ($MgCl_2$)	45

2.3 Temperature Calibration

According to Eq. (1), both strain and temperature variations also influence the Bragg wavelength shift. This indicates that temperature affects the Bragg wavelength simultaneously with applied strain. Therefore, it is crucial to calibrate the temperature effects on the FBGs by maintaining a constant strain value. To achieve this, the humidity level was fixed at 100% by submerging the coated multiplexed FBG sensor in a water bath while the temperature was varied from 10 °C to 40 °C. Temperature calibration was conducted using a water bath manufactured by FAITHFUL Instrument, model FC-0530 Low-Temperature Circulation Bath, to ensure precise temperature control. The entire sensor was submerged in a water bath, starting at 10 °C, with increments of 10 °C until it reached 40 °C. As illustrated in Figure 3, the experimental setup incorporated a BLS, an OSA, and an optical fibre circulator. These components facilitated real-time monitoring of the sensor's response, enabling calibration and sensitivity analysis of the coated multiplexed sensor with respect to temperature variations. The data measurement was also repeated three times to obtain an average result in this calibration.

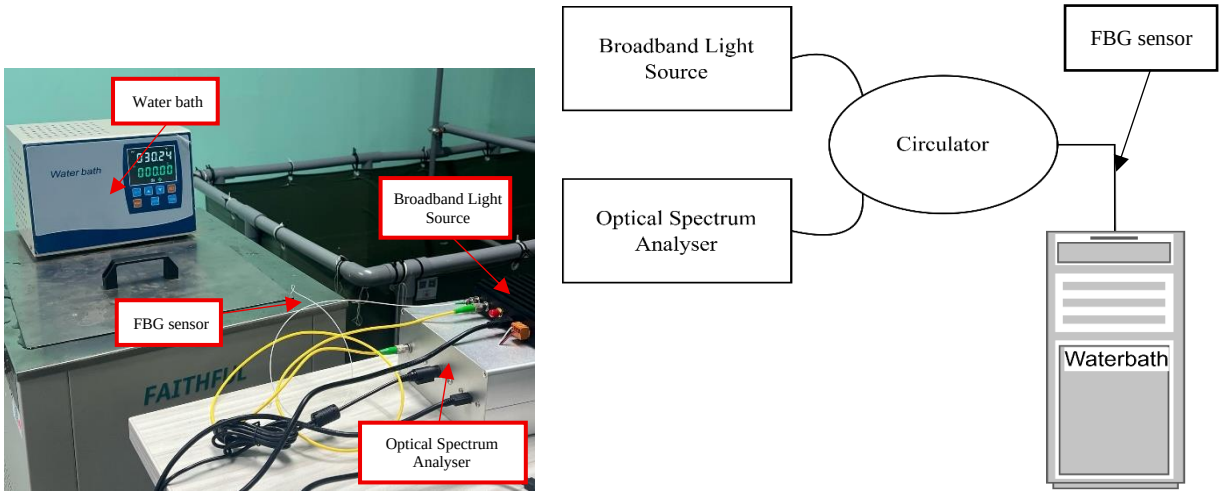

Figure 3. Actual and schematic experiment setup of temperature calibration

2.4 Simultaneous Humidity and Temperature Measurement

Once the relative humidity and temperature were calibrated, a simultaneous measurement experiment for both parameters was conducted using the setup illustrated in Figure 4. Before starting the experiment, the ambient laboratory temperature was recorded at 29 °C using a thermo-hygrometer. The experimental setup was positioned directly beneath the air-conditioner to ensure exposure to cooled air. Prior to data collection, both the humidifier and air-conditioner were activated simultaneously, and real-time humidity and temperature measurements were recorded using the thermo-hygrometer. The initial temperature of 29 °C was gradually reduced to 22 °C by rapidly cooling the room. Humidity levels were controlled using a humidifier, allowing variations from 80% RH to 99% RH. The coated multiplexed FBG sensor was exposed to these controlled environmental conditions to monitor wavelength shifts in response to simultaneous changes in humidity and temperature. The primary objective of this calibration was to evaluate the sensor's accuracy in measuring both parameters concurrently.

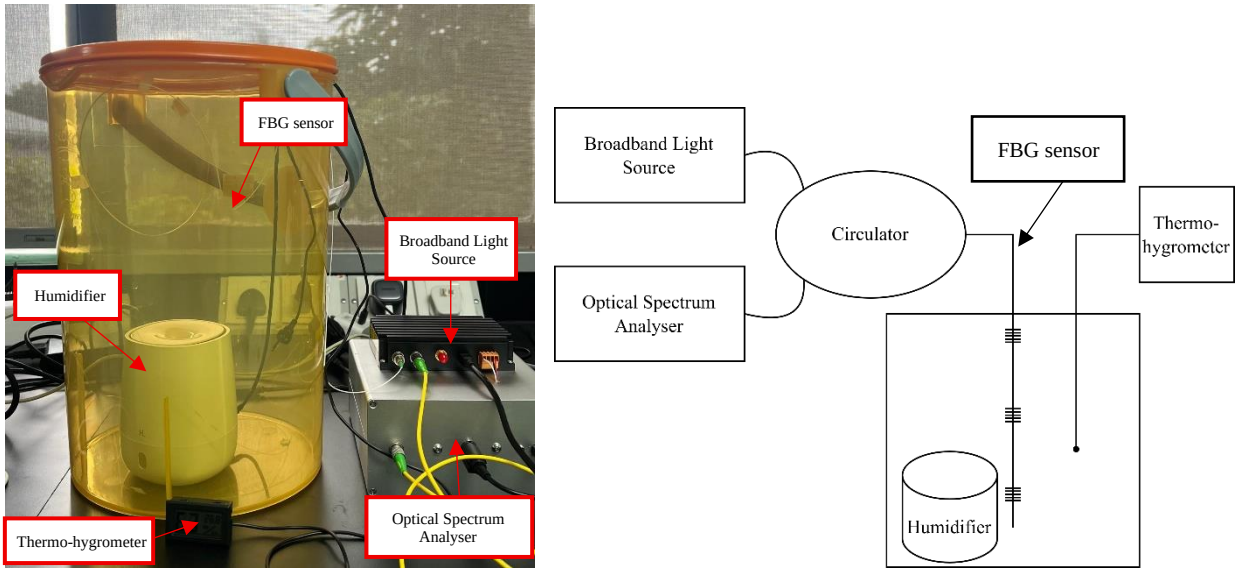

Figure 4. Actual and schematic experimental setup of simultaneous humidity and temperature calibration

3. RESULTS AND DISCUSSION

3.1 Reflection Spectrum

Figure 5 presents the reflection spectra of the PDMS-coated and PVA-coated FBGs. Figure 5(a) illustrates the centre wavelength of the PDMS-coated FBG, recorded at 1548.7644 nm before coating and 1548.7474 nm after the coating process. Similarly, Figure 5(b) compares the centre wavelength of the PVA-coated FBG measured at 1553.4000 nm before coating and 1553.3280 nm after coating. The observed spectral shifts indicate changes in the grating period due to strain induced by the coating materials. The strain results from the bonding force of the coating, which exerts a compression effect on the fibre grating, leading to a shift in the reflected wavelength [24]. The blueshift observed after coating the FBG demonstrates the strain applied by the PVA layer. Notably, the wavelength reduction in Figure 5(a) is minimal compared to Figure 5(b), suggesting a more pronounced strain effect from the PVA coating.

Table 2 summarises the wavelength shifts and percentage differences for both coatings, revealing that PVA induces a greater wavelength shift than PDMS. This finding indicates that PVA exerts more strain on the grating period compared to PDMS during the curing process. The greater strain from the PVA coating is likely due to the hydrophilic nature and curing behavior of PVA. As the water content in PVA evaporates during drying, the material undergoes shrinkage, resulting in compressive stress on the fibers [25]. Furthermore, PVA forms hydrogen bonds with the silica surface, which enhances mechanical coupling [26]. In contrast, PDMS, being more elastic and hydrophobic [27], exerts less compressive force due to its minimal shrinkage and weaker surface interaction with the fibre.

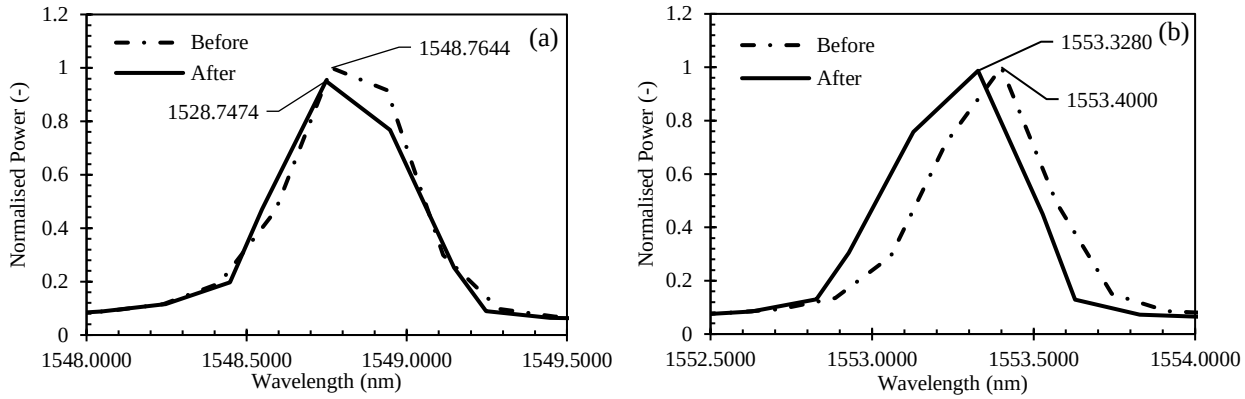

Figure 5. Reflection spectrum comparison of: (a) PDMS-coated and (b) PVA-coated FBG

Table 2. PDMS and PVA spectrum wavelength change

Coating	Before (nm)	After (nm)	Difference	Percent difference
Polydimethylsiloxane (PDMS)	1548.7644	1548.7474	0.017	0.001098
Polyvinyl alcohol (PVA)	1553.4000	1553.3280	0.072	0.004635

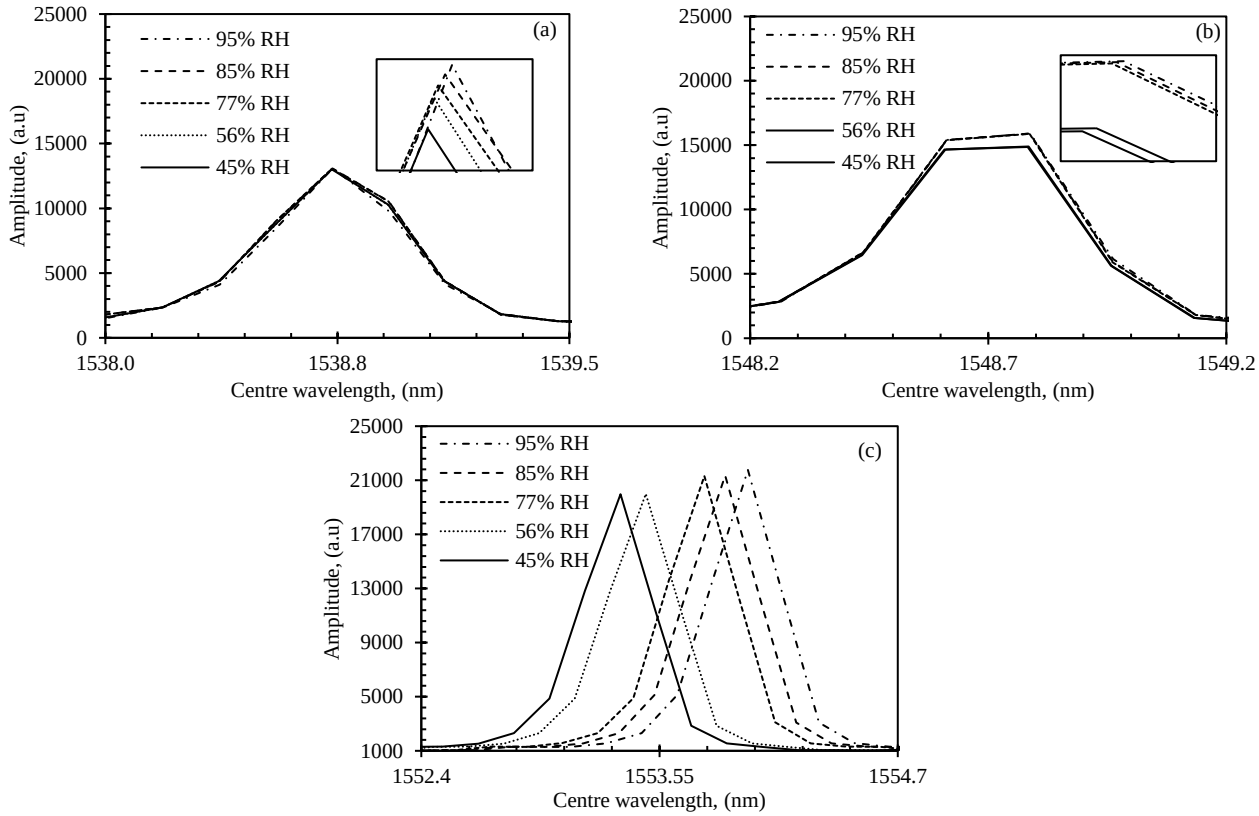

Figure 6. First increase centre wavelength in the relative humidity experiment for: (a) bare, (b) PDMS-coated, and (c) PVA-coated FBG

3.2 Relative Humidity Calibration Results

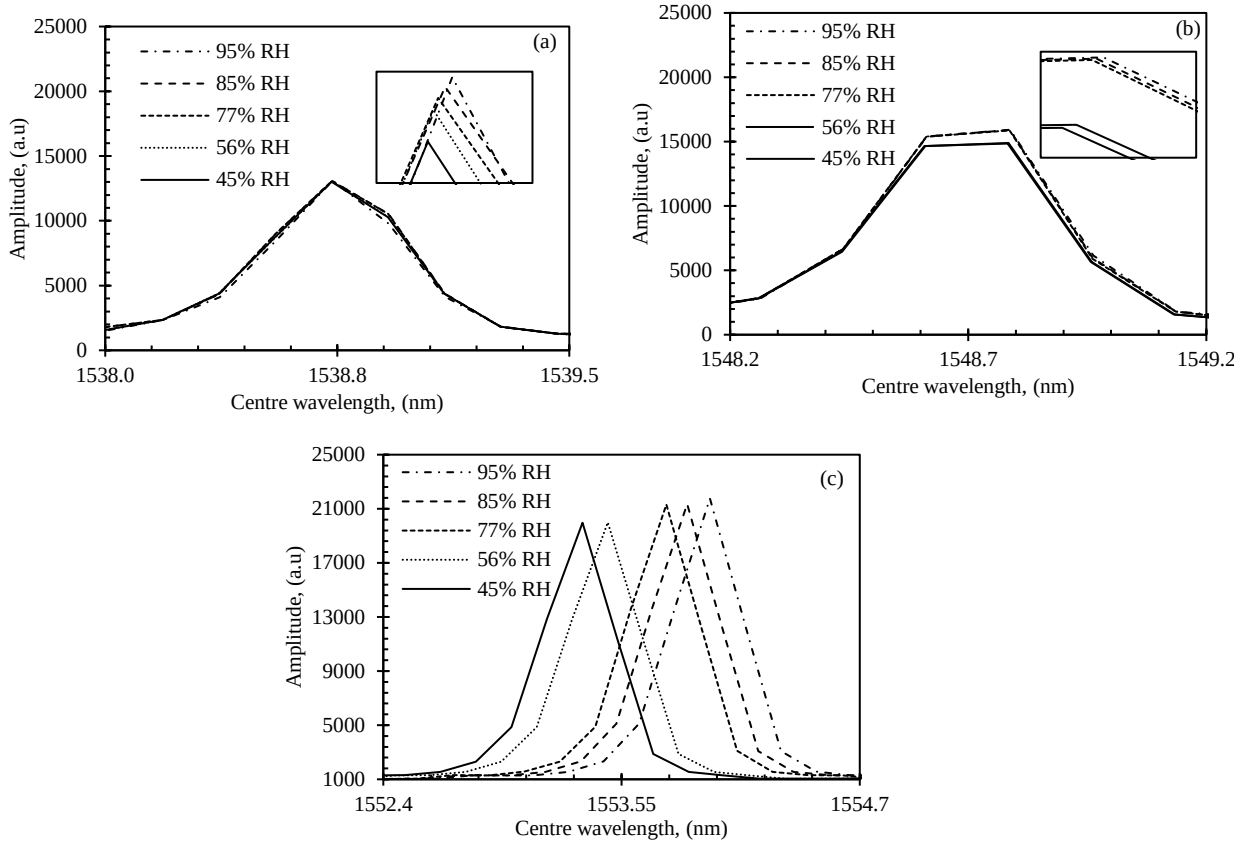

Figure 6 presents the first increase in centre wavelength shift obtained for each RH level from the salt solution experiment. The RH range varied from 45% RH to 95% RH, where a clear redshift in the centre wavelength was observed with increasing humidity. For the PVA-coated FBG, the centre wavelength increased from 1553.3553 nm to 1553.9801 nm, resulting in a total wavelength shift of 0.6248 nm. In contrast, the PDMS-coated FBG exhibited minimal wavelength shifts, indicating a weak response to humidity, as reported in [14]. The centre wavelength variation ranged from 1548.7815 nm to 1548.7889 nm, corresponding to a total shift of 0.0074 nm. Similarly, the bare FBG showed negligible sensitivity to humidity, with a total wavelength shift of only 0.0052 nm. After applying a humidity-sensitive PVA coating to the bare FBG, its sensitivity was enhanced by approximately 219.2 times, demonstrating the significant impact of the coating on humidity detection.

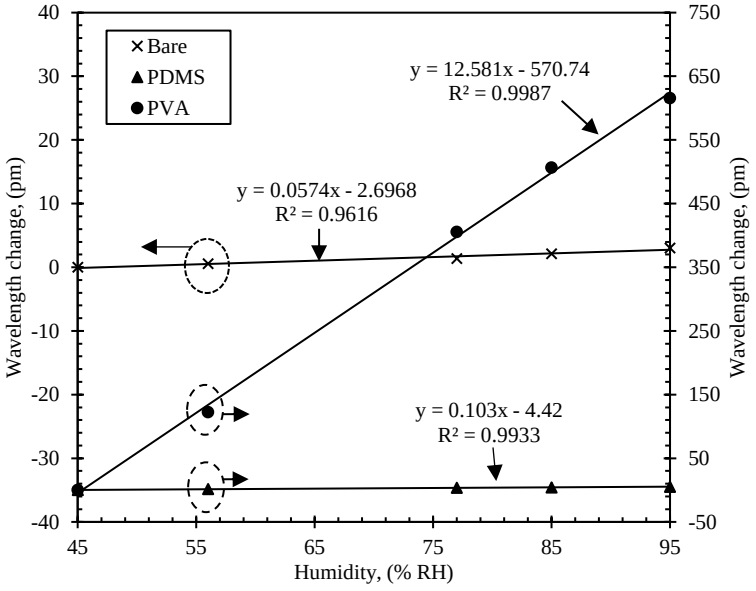

Figure 7. Relative humidity sensitivity of coated multiplexed FBG sensor

Table 3 displays the average centre wavelength values corresponding to each RH level obtained from the salt solution experiment. From these values, the RH sensitivity of the coated multiplexed sensor was determined. Figure 7 illustrates the RH sensitivities, where the PVA-coated FBG exhibited a higher sensitivity of 12.581 pm/% RH compared to the

PDMS-coated and bare FBGs, which had sensitivities of 0.103 pm/% RH and 0.0574 pm/% RH, respectively. The linear regression of the PVA-coated FBG reveals that the center wavelength shift is highly dependent on relative humidity, with a strong correlation coefficient of 0.9987. Figure 8 shows the Bragg wavelength shift and its standard deviation error bar for each FBG. PVA, being hydrophilic, shows results that are mostly within the standard deviation. Its hysteresis is within the range of ±0.006 nm, demonstrating good repeatability and sensitivity towards humidity. Although bare FBG and PDMS-coated FBG show results that coincide with each other, demonstrating good repeatability, their standard deviation of ±0.00028 nm indicates a lack of reaction to humidity.

Table 3. Average centre wavelength values obtained from relative humidity calibration

Coated FBG	Average centre wavelength (nm)				
	45% RH	56% RH	77% RH	85% RH	95% RH
Bare	1538.7311	1538.7317	1538.7325	1538.7332	1538.7341
Polydimethylsiloxane (PDMS)	1548.7824	1548.7840	1548.7859	1548.7866	1548.7877
Polyvinyl alcohol (PVA)	1553.3583	1553.4807	1553.7636	1553.8650	1553.9741

3.3 Temperature Calibration Results

Figure 9 presents the centre wavelength variations as a function of temperature, where the sensor was fully immersed in a water bath. The temperature was controlled within a range of 10°C to 40°C, and the centre wavelength exhibited a redshift as the temperature increased. For the PVA-coated FBG, the wavelength shifted from 1553.1573 nm to 1553.6918 nm, resulting in a total shift of 0.5345 nm. Meanwhile, for the PDMS-coated FBG, the centre wavelength increased from 1548.5903 nm to 1549.5482 nm, corresponding to a total shift of 0.9579 nm, which is nearly twice the shift observed in the PVA-coated FBG. This significant change in PDMS-coated FBG suggests its superior thermal detection capabilities. According to Wang et al. [28], PDMS has a large thermal expansion coefficient, which improves the sensitivity of the fibre. Additionally, Zhang et al. [29] reported that at higher temperatures, PDMS exhibits greater compressive behavior, although their study focused on cryogenic conditions. As described in Eq. (1), the expansion of the coating material induces strain on the grating period, resulting in changes to the Bragg wavelength.

3.4 Simultaneous Humidity and Temperature Measurement Results

As observed in Figure 10, FBGs are inherently influenced by temperature variations, even when coated with a material primarily designed for humidity sensing. This interaction may introduce cross-sensitivity, potentially affecting the accuracy of the results. To address this, the sensitivity coefficients obtained from the calibration were used to formulate the sensitivity coefficient matrix, which can be expressed as:

$$\begin{bmatrix}\Delta\lambda_{PVA}\\ \Delta\lambda_{PDMS}\end{bmatrix}=\begin{bmatrix}S_{RHPVA} & S_{TPVA}\\ S_{RHPDMS} & S_{TPDMS}\end{bmatrix}\begin{bmatrix}\Delta RH\\ \Delta T\end{bmatrix} \quad (3)$$

where $\Delta\lambda_{PVA}$ and $\Delta\lambda_{PDMS}$ are the wavelength shifts of the two types of coated FBG materials. S_{RHPVA} and S_{TPVA} are the relative humidity and temperature sensitivities of $\Delta\lambda_{PVA}$. Meanwhile, S_{RHPDMS} and S_{TPDMS} are the relative humidity and temperature sensitivities of $\Delta\lambda_{PDMS}$. ΔRH and ΔT are the changes in humidity and temperature, respectively. Therefore, the matrix can be expressed as:

$$\begin{bmatrix}\Delta\lambda_{PVA}\\ \Delta\lambda_{PDMS}\end{bmatrix}=\begin{bmatrix}12.581 & 14.471\\ 0.103 & 28.524\end{bmatrix}\begin{bmatrix}\Delta RH\\ \Delta T\end{bmatrix} \quad (4)$$

presents the recorded average centre wavelength for each temperature increment. From these values, the temperature sensitivity of the coated multiplexed sensor was calculated. Figure 10 illustrates the obtained temperature sensitivities of 28.524 pm/°C for the PDMS-coated FBG and 14.471 pm/°C for the PVA-coated FBG, both demonstrating excellent linearity with R^2 = 0.9968 and R^2 = 0.9966, respectively. For comparison, the bare FBG exhibited a centre wavelength from 1538.5618 nm to 1538.9298 nm, with a total shift of 0.368 nm and a temperature sensitivity of 11.230 pm/°C. These results indicate that the PDMS-coated FBG and PVA-coated FBG achieved approximately 2.54 times and 1.29 times higher temperature sensitivity, respectively, compared to the bare FBG. This confirms that the coated FBG exhibited higher temperature sensitivity compared to the bare FBG due to its increased thermal expansion coefficient. Figure 11 (a-c) shows the wavelength shift difference as a function of the applied temperature, exhibiting a linear pattern. The results coincide with each other, demonstrating that the temperature calibration has good repeatability. Figure 11 (d-f) presents the standard deviation error of the results obtained in Figure 11 (a-c), respectively. PDMS, with a good thermal expansion recovery time, exhibits a slight hysteresis at ±0.00418 nm, with the lowest value at ±0.00244 nm. These results confirm the properties of PDMS, showing good dynamic response over repeated thermal cycles. The maximum hysteresis from the temperature calibration was ±0.00608 nm, and the lowest was at ±0.00144 nm. This represents a good thermal response and an excellent repeatability over a dynamic range of more than 400 pm.

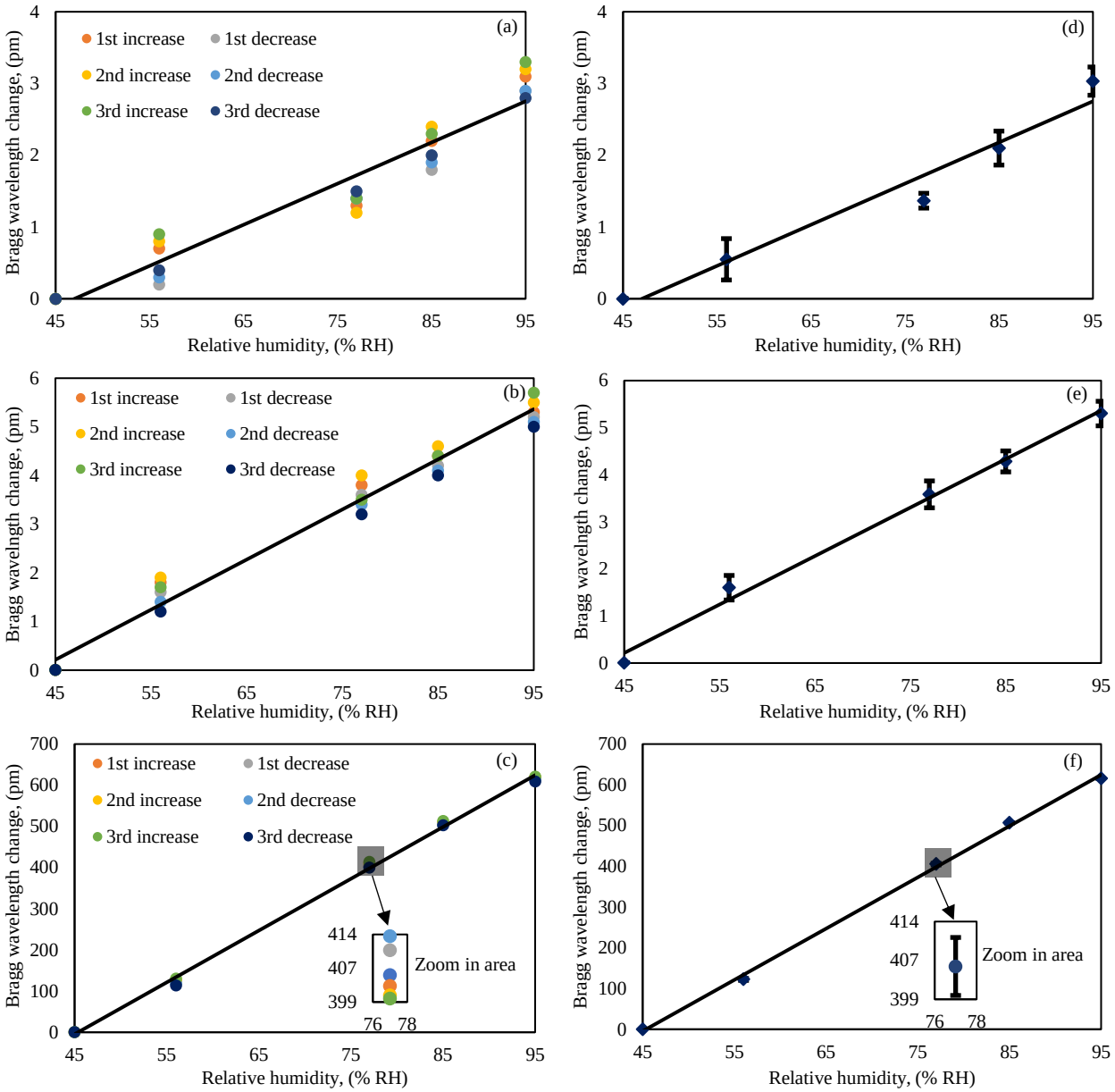

Figure 8. Humidity Bragg wavelength shift difference for: (a) bare, (b) PDMS-coated, and (c) PVA-coated FBGs, and its (d) (e) (f) respective standard deviation error bar

Table 4. Average centre wavelength values obtained from temperature calibration

Coated FBG	Centre wavelength (nm)			
	10°C	20°C	30°C	40°C
Bare	1538.5766	1538.6720	1538.7767	1538.9145
Polydimethylsiloxane (PDMS)	1548.6337	1548.8976	1549.1646	1549.4972
Polyvinyl alcohol (PVA)	1553.2082	1553.3712	1553.5171	1553.6435

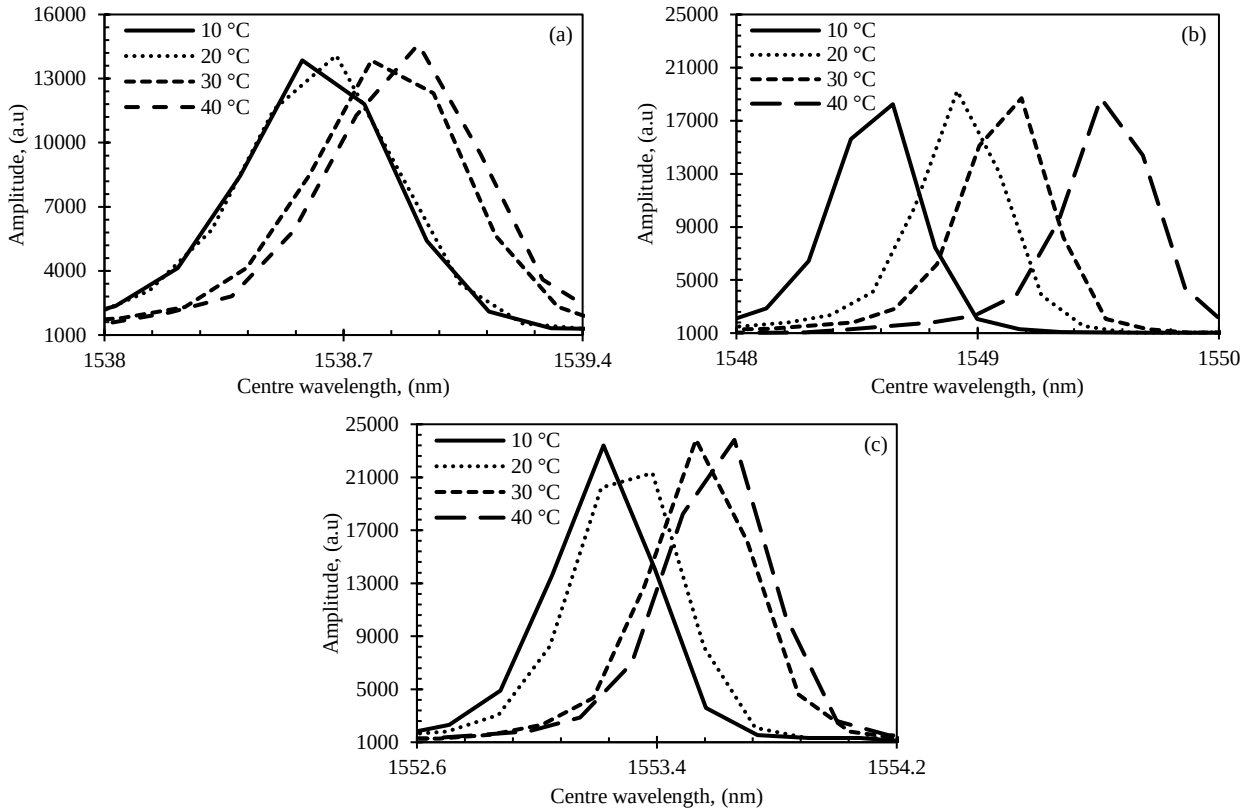

Figure 9. First increase centre wavelength in temperature experiment for: (a) bare, (b) PDMS coated, and (c) PVA coated FBG

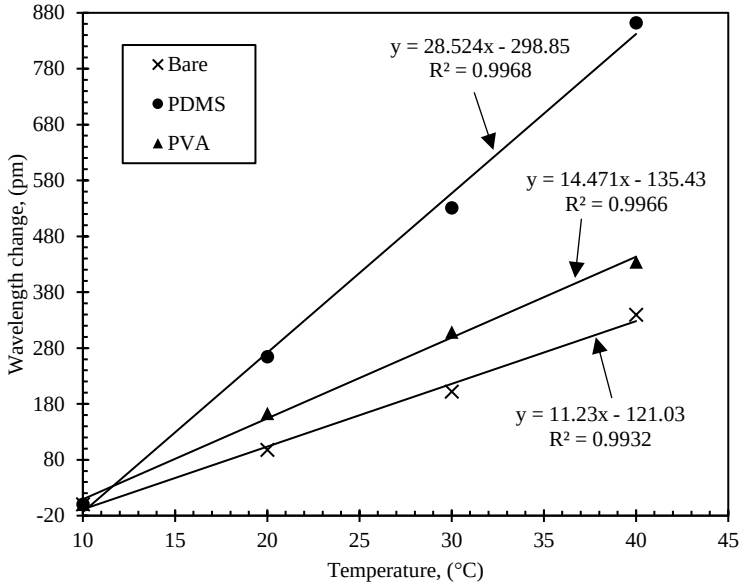

Figure 10. Temperature sensitivity of coated multiplexed FBG sensor

3.4 Simultaneous Humidity and Temperature Measurement Results

As observed in Figure 10, FBGs are inherently influenced by temperature variations, even when coated with a material primarily designed for humidity sensing. This interaction may introduce cross-sensitivity, potentially affecting the accuracy of the results. To address this, the sensitivity coefficients obtained from the calibration were used to formulate the sensitivity coefficient matrix, which can be expressed as:

$$\begin{bmatrix} \Delta\lambda_{PVA} \\ \Delta\lambda_{PDMS} \end{bmatrix} = \begin{bmatrix} S_{RHPVA} & S_{TPVA} \\ S_{RHPDMS} & S_{TPDMS} \end{bmatrix} \begin{bmatrix} \Delta RH \\ \Delta T \end{bmatrix} \quad (3)$$

where $\Delta\lambda_{PVA}$ and $\Delta\lambda_{PDMS}$ are the wavelength shifts of the two types of coated FBG materials. S_{RHPVA} and S_{TPVA} are the relative humidity and temperature sensitivities of $\Delta\lambda_{PVA}$. Meanwhile, S_{RHPDMS} and S_{TPDMS} are the relative humidity and

temperature sensitivities of $\Delta\lambda_{PDMS}$. ΔRH and ΔT are the changes in humidity and temperature, respectively. Therefore, the matrix can be expressed as:

$$\begin{bmatrix}\Delta\lambda_{PVA}\\ \Delta\lambda_{PDMS}\end{bmatrix} = \begin{bmatrix}12.581 & 14.471\\ 0.103 & 28.524\end{bmatrix}\begin{bmatrix}\Delta RH\\ \Delta T\end{bmatrix} \tag{4}$$

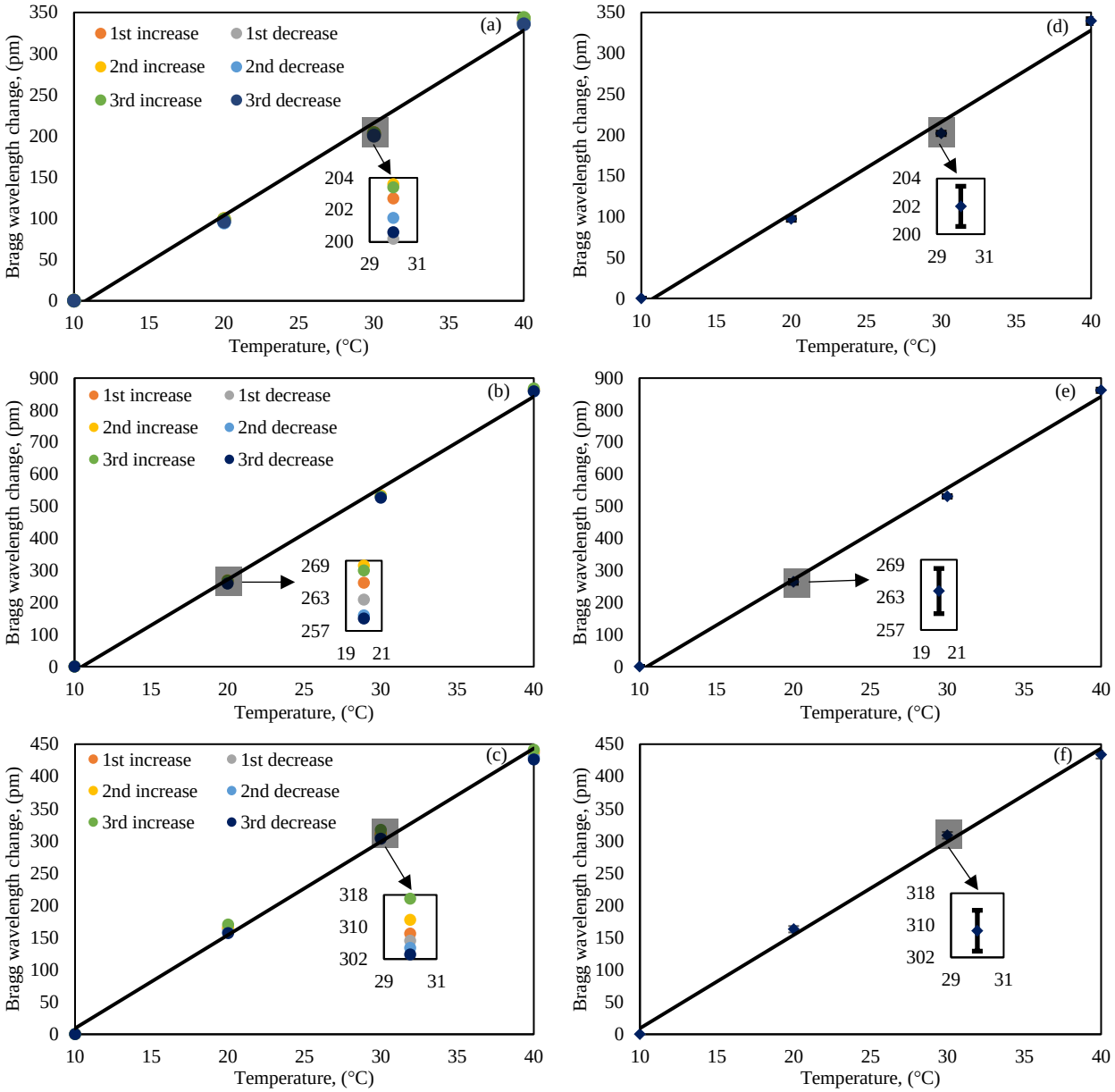

Figure 11. Temperature Bragg wavelength shift difference for: (a) bare, (b) PDMS-coated, and (c) PVA-coated FBGs and their (d) (e) (f) respective standard deviation error bar

By inversing Eq. (4), the relative humidity change and temperature change matrix can be expressed as:

$$\begin{bmatrix}\Delta RH\\ \Delta T\end{bmatrix} = \begin{bmatrix}0.0799 & -0.0405\\ -0.000288 & 0.0352\end{bmatrix}^{-1}\begin{bmatrix}\Delta\lambda_{PVA}\\ \Delta\lambda_{PDMS}\end{bmatrix} \tag{5}$$

By expanding Eq. (5), the simultaneous measurement of relative humidity and temperature can be expressed as:

$$RH_f = [0.0799 \cdot \Delta\lambda_{PVA} + -0.0405 \cdot \Delta\lambda_{PDMS}] + RH_i \tag{6}$$

$$T_f = [-0.000288 \cdot \Delta\lambda_{PVA} + 0.0352 \cdot \Delta\lambda_{PDMS}] + T_i \tag{7}$$

where, RH_f is the final relative humidity and RH_i is the initial relative humidity. T_f is the final temperature and T_i is the initial temperature. The relative humidity and temperature values estimated by the coated FBGs were compared with the actual values, and the percentage error was calculated.

Figure 12 presents the percentage error by comparing the actual and estimated values for relative humidity and temperature measurements. As shown in Figure 12(a) and Figure 12(b), the maximum percentage errors recorded for relative humidity and temperature were 9.7% and 9.9%, respectively. The values indicate an acceptable error range of less than 10%, demonstrating the reliability of the proposed sensor.

Table 5 and Table 6 provide a detailed comparison of the actual and estimated humidity and temperature measurements, along with the corresponding percentage errors under various experimental conditions. The factors that affect the error percentage are mainly due to the material used for coating the FBGs. PVA being hygroscopic, experiences swelling or saturation, especially at very high humidity levels. This would cause inconsistent strain transmission to the fibre as the humidity level increases. PDMS exhibits a slower thermal response at lower temperatures due to its viscoelastic nature, which introduces a lag in equilibrium. A material at maximum saturation would exhibit uneven swelling, which causes a lag in simultaneous measurements. Hence, there is an error in the measurements, resulting in consistently lower estimated temperatures compared to the actual temperatures.

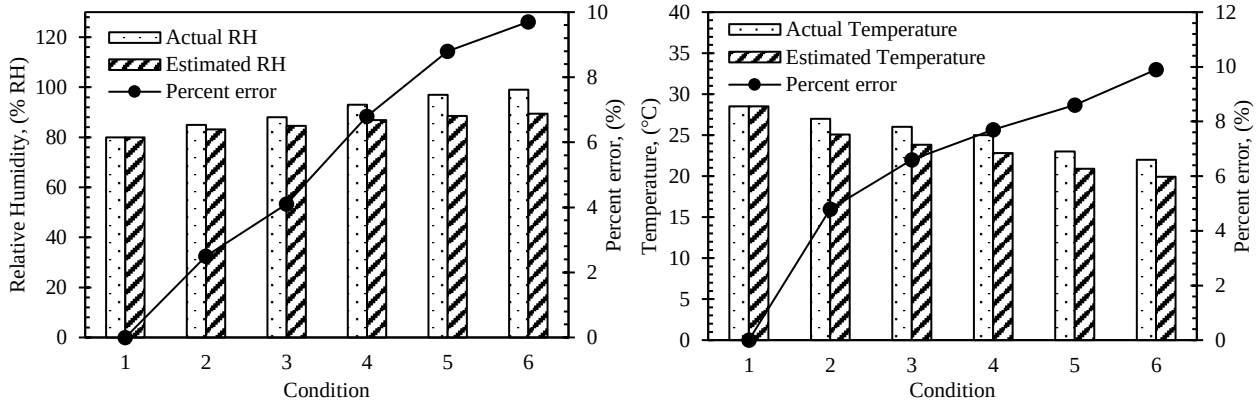

Figure 12. Percentage error for: (a) RH experiment and (b) Temperature experiment

Table 5. Relative humidity accuracy measurement

Condition	Actual RH (% RH)	Estimated RH (% RH)	Percentage error (%)
1	80	80.0	0
2	85	82.8	2.5
3	88	84.4	4.1
4	93	86.7	6.8
5	97	88.4	8.8
6	99	89.4	9.7

Table 6. Temperature accuracy measurement

Condition	Actual temperature (°C)	Estimated temperature (°C)	Percentage error (%)
1	28.5	28.5	0
2	27.0	25.7	4.8
3	26.0	24.3	6.6
4	25.0	23.1	7.7
5	23.0	21.0	8.6
6	22.0	19.8	9.9

4. CONCLUSIONS

The objective of developing a simple and effective sensor for simultaneous humidity and temperature measurement using coated multiplexed FBGs was successfully achieved, with a percentage error of below 10%. The fabrication process was straightforward and did not require specialised or advanced equipment, making the proposed sensor highly accessible for practical applications. The sensitivity analysis confirmed that the PVA-coated FBG exhibited sensitivities of 12.581 pm/% RH for humidity and 14.471 pm/°C for temperature. In comparison, the PDMS-coated FBG demonstrated 0.103 pm/% RH for humidity and 28.524 pm/°C for temperature. These findings validate the suitability of PVA and PDMS coatings for humidity and temperature sensing applications, respectively. Furthermore, the sensor calibration yielded results within a 10% error margin, demonstrating good accuracy. Additionally, the standard deviation for both temperature and humidity calibration does not exceed ±0.00608 ppm, indicating moderate hysteresis and good repeatability for

humidity and temperature sensors. The issue of cross-sensitivity, a common challenge in simultaneous measurements, was effectively mitigated through the application of sensitivity matrices, ensuring reliable and accurate readings. Overall, this study establishes the feasibility of a cost-effective, reliable, and accurate coated multiplexed FBG sensor for simultaneous measurement of humidity and temperature, offering a promising solution for optical fibre sensing applications.

ACKNOWLEDGEMENTS

This work was supported by Yayasan UTP Fundamental Research Grant (YUTP-FRG) allocated under the cost centre 015LC0-542. The authors would also like to thank Universiti Teknologi PETRONAS (UTP), the Institute of Smart & Sustainable Living (ISSL), and the Centre of Smart Infrastructure Modelling & Monitoring (SIMM) for their support in this research.

CONFLICT OF INTEREST

The authors declare that they have no conflicts of interest.

AUTHORS CONTRIBUTION

A. R. Azmi (Methodology; Data curation; Formal analysis; Investigation; Visualisation; Writing - original draft)

A. M. Aizzuddin (Methodology; Data curation; Formal analysis; Investigation; Visualisation; Writing - original draft)

E. Vorathin (Validation; Writing - review & editing; Funding acquisition; Supervision)

K. S. Lim (Conceptualisation; Methodology; Supervision)

M. Mohammad (Resources; Software; Supervision)

A. R. Othman (Resources; Project Administration)

A. R. Ismail (Resources; Software)

AVAILABILITY OF DATA AND MATERIALS

The data supporting this study's findings are available on request from the corresponding author and can be shared upon reasonable request.

ETHICS STATEMENT

The authors confirm that AI or AI-aided technologies have been listed as an author or co-author on this manuscript. The authors fully understand the role of authorship and its associated responsibilities and obligations, which can only be fulfilled by humans. The preparation of this manuscript has been under these guidelines.

REFERENCES

[1] W. Zhang, M. Awais, S. M. Z. A. Naqvi, Y. Xiong, L. Li, Y. Zang, et al., "Real-time remote corn growth monitoring system using plant wearable fiber Bragg grating sensor," *Computers and Electronics in Agriculture*, vol. 227, p. 109538, 2024.

[2] D. Krizan, J. Stipal, J. Nedoma, S. Oliveira, M. Fajkus, J. Cubik, et al., "Embedding FBG sensors for monitoring vital signs of the human body: Recent progress over the past decade," *APL Photonics*, vol. 9, no. 8, 2024.

[3] X. Su, Y. Geng, L. Huang, S. Li, Q. Wang, Z. Xu, et al., "Review on dehumidification technology in low and extremely low humidity industrial environments," *Energy*, vol. 302, p. 131793, 2024.

[4] Z. Wang, M. Cao, H. Tang, B. Dong, Y. Ji, F. Han, "Marine temperature and humidity regulation combined system: Performance analysis and multi-objective optimization," *Case Studies in Thermal Engineering*, vol. 56, p. 104215, 2024.

[5] M. H. Yassin, M. H. Farhat, R. Soleimanpour, M. Nahas, "Fiber Bragg grating (FBG)-based sensors: a review of technology and recent applications in structural health monitoring (SHM) of civil engineering structures," *Discover Civil Engineering*, vol. 1, no. 1, pp. 1-39, 2024.

[6] Y. Zhang, Y. Li, Z. Guo, J. Li, X. Ge, Q. Sun, et al., "Health monitoring by optical fiber sensing technology for rechargeable batteries," *eScience*, vol. 4, no. 1, p. 100174, 2024.

[7] C. Lu, Z. Chen, D. Zeng, J. Lin, C. Wu, "Fast-response temperature sensing using dual-wavelength differential cross multiplication for interrogating fiber-optic fabry-pérot interferometers," *IEEE Sensors Journal*, vol. 24, no. 6, pp. 9633-9640, 2025.

[8] Z. Han, J. Chao, Z. Xiping, W. Pei, C. Tingshui, L. Changning, et al., "Simultaneous humidity and temperature measurement sensor based on two cascaded long-period fiber gratings," *Optics Communications*, vol. 530, p. 129137, 2023.

[9] R.-j. Tong, Y. Zhao, H.-k. Zheng, F. Xia, "Simultaneous measurement of temperature and relative humidity by compact Mach-Zehnder interferometer and Fabry-Perot interferometer," *Measurement*, vol. 155, p. 107499, 2020.

[10] E. Vorathin, Z. M. Hafizi, N. Ismail, M. Loman, "Review of high sensitivity fibre-optic pressure sensors for low pressure sensing," *Optics & Laser Technology*, vol. 121, p. 105841, 2020.

[11] Y. Qi, C. Jia, L. Tang, X. Zhang, C. Gong, Y. Liu, et al., "Research on temperature and humidity sensing characteristics of cascaded LPFG-FBG," *Optik*, vol. 188, pp. 19-26, 2019.

[12] T. Cheng, B. Li, F. Zhang, W. Liu, X. Chen, Y. Gao, et al., "Simultaneous measurement of ultraviolet irradiance and temperature by employing optical fiber SPR sensor with Ag/ZnO/PDMS coating," in *IEEE Transactions on Instrumentation and Measurement*, vol. 72, pp. 1-8, 2023.

[13] H. Fan, Y. Bao, H. Guo, Y. Sun, L. Fan, "Polymeric microwire-enabled fiber Bragg grating for simultaneous humidity and temperature sensing," *IEEE Sensors Journal*, vol. 24, no. 3, pp. 2779-2784, 2023.

[14] Y. Zhang, J. Yu, P. Liu, C. Liu, X. Tang, Z. Liu, et al., "All-fiber temperature and humidity sensor based on photopolymer and polydimethylsiloxane with low-crosstalk and high-sensitivity," *Optical Fiber Technology*, vol. 80, p. 103410, 2023.

[15] Y. Xu, X. Zhao, Y. Li, Z. Qin, Y. Pang, Z. Liu, "Simultaneous measurement of relative humidity and temperature based on forward Brillouin scattering in polyimide-overlaid fiber," *Sensors and Actuators B: Chemical*, vol. 348, p. 130702, 2021.

[16] Z. Qin, S. Qu, Z. Wang, W. Yang, S. Li, Z. Liu, et al., "A fully distributed fiber optic sensor for simultaneous relative humidity and temperature measurement with polyimide-coated polarization maintaining fiber," *Sensors and Actuators B: Chemical*, vol. 373, p. 132699, 2022.

[17] N. Chen, C. Liu, L. Chen, L. Yang, "Femtosecond laser-inscribed fiber-optic sensor for simultaneous temperature and relative humidity measurements," *Optics & Laser Technology*, vol. 164, p. 109463, 2023.

[18] D. Liu, Z. Cai, B. Li, M. Zou, L. Zhang, Y. Hua, et al., "Simultaneous measurement of humidity and temperature based on fiber-tip microcantilever cascaded with fiber Bragg grating," *Optics Express*, vol. 31, no. 5, pp. 8738-8747, 2023.

[19] Z. Wang, L. Li, Q. Ma, M. Wang, W. Wei, P. Yang, et al., "Loop-Fiber coated with graphene oxide incorporating a FBG to sense humidity and temperature simultaneously," *Optics Communications*, vol. 508, p. 127819, 2022.

[20] M. Elsherif, A. E. Salih, M. G. Muñoz, F. Alam, B. AlQattan, D. S. Antonysamy, et al., "Optical fiber sensors: Working principle, applications, and limitations," *Advanced Photonics Research*, vol. 3, no. 11, p. 2100371, 2022.

[21] S. Korganbayev, T. Ayupova, M. Sypabekova, A. Bekmurzayeva, M. Shaimerdenova, K. Dukenbayev, et al., "Partially etched chirped fiber bragg grating (pECFBG) for joint temperature, thermal profile, and refractive index detection," *Optics Express*, vol. 26, no. 14, pp. 18708-18720, 2018.

[22] Z. Liang, D. Liu, X. Wang, J. Zhang, H. Wu, X. Qing, et al., "FBG-based strain monitoring and temperature compensation for composite tank," *Aerospace Science and Technology*, vol. 127, p. 107724, 2022.

[23] L. Greenspan, "Humidity fixed points of binary saturated aqueous solutions," *Journal of Research of the National Bureau of Standards. Section A, Physics and Chemistry*, vol. 81, no. 1, p. 89, 1977.

[24] X. Li, M. Zheng, D. Hou, Q. Wen, "Advantageous strain sensing performances of FBG strain sensors equipped with planar UV-curable resin," *Sensors*, vol. 23, no. 5, p. 2811, 2023.

[25] J. T. L. Yeo, "Application of FBG-based sensors in build environment," *PhD Thesis*, University of London, 2007.

[26] H. Pingan, J. Mengjun, Z. Yanyan, H. Ling, "A silica/PVA adhesive hybrid material with high transparency, thermostability and mechanical strength," *RSC Advances*, vol. 7, no. 5, pp. 2450-2459, 2017.

[27] S. Sun, Y. Huang, B. Zhao, "Formation of silica colloidal crystals on soft hydrophobic vs rigid hydrophilic surfaces," *Colloids and Surfaces A: Physicochemical and Engineering Aspects*, vol. 467, pp. 180-187, 2015.

[28] Z. Wang, D. Chen, X. Yang, S. Liang, X. Sun, "Temperature sensor of single-mode-no-core-single-mode fiber structure coated with PDMS," *Optical Fiber Technology*, vol. 68, p. 102793, 2022.

[29] G. Zhang, Y. Sun, B. Qian, H. Gao, D. Zuo, "Experimental study on mechanical performance of polydimethylsiloxane (PDMS) at various temperatures," *Polymer Testing*, vol. 90, p. 106670, 2020.